

The brighter galaxies reionised the Universe

Mahavir Sharma^{1*}, Tom Theuns¹, Carlos Frenk¹, Richard Bower¹, Robert Crain²,
Matthieu Schaller¹ & Joop Schaye³

¹ *Institute for Computational Cosmology, Department of Physics, University of Durham, South Road, Durham, DH1 3LE, UK*

² *Astrophysics Research Institute, Liverpool John Moores University, 146 Brownlow Hill, Liverpool L3 5RF, UK*

³ *Leiden Observatory, Leiden University, P.O. Box 9513, 2300 RA Leiden, the Netherlands*

18 October 2018

ABSTRACT

Hydrogen in the Universe was (re)ionised between redshifts $z \approx 10$ and $z \approx 6$. The nature of the sources of the ionising radiation is hotly debated, with faint galaxies below current detection limits regarded as prime candidates. Here we consider a scenario in which ionising photons escape through channels punctured in the interstellar medium by outflows powered by starbursts. We take account of the observation that strong outflows occur only when the star formation density is sufficiently high, and estimate the galaxy-averaged escape fraction as a function of redshift and luminosity from the resolved star formation surface densities in the EAGLE cosmological hydrodynamical simulation. We find that the fraction of ionising photons that escape from galaxies increases rapidly with redshift, reaching values of 5–20 per cent at $z > 6$, with the brighter galaxies having higher escape fractions. Combining the dependence of escape fraction on luminosity and redshift with the observed luminosity function, we demonstrate that galaxies emit enough ionising photons to match the existing constraints on reionisation while also matching the observed UV-background post-reionisation. Our findings suggest that galaxies above the current *Hubble Space Telescope* detection limit emit half of the ionising radiation required to reionise the Universe.

Key words: dark ages, reionisation – Galaxies : starburst

1 INTRODUCTION

Consensus is emerging that neutral hydrogen in the Universe was (re)ionised between redshifts $z \approx 10$ and $z \approx 6$ (e.g. Robertson et al. 2015; McGreer et al. 2015; Mitra et al. 2015). The nature of the sources of the ionising radiation has not yet been firmly established, but attention has focussed on an early generation of galaxies. Regions around such galaxies are ionised first, and these ionised bubbles grow in number and size until they percolate as more and brighter galaxies form (Gnedin 2000; Shin et al. 2008). Therefore, as reionisation proceeds, a larger fraction of the Universe becomes ionised (see e.g. Loeb & Barkana (2001) for a review).

A crucial factor in modelling reionisation is the fraction of ionising photons that escape their natal galaxy, f_{esc} . Neutral hydrogen and dust in the interstellar medium (ISM) and circumgalactic medium (CGM) determine a galaxy’s f_{esc} . This quantity is difficult to measure and observational claims of the detection of ionising photons escaping from galaxies are controversial. The value of f_{esc} is often assumed to be constant (e.g. Bouwens et al. 2011; Robertson et al. 2013) or increasing towards lower luminosities (e.g. Ferrara & Loeb 2013). In such models, faint galaxies far below current detection limits dominate the ionising emissivity.

Observed values of f_{esc} at $z \approx 0$ are generally a few per cent or less. For example, Bland-Hawthorn & Maloney (2001) infer a value of $f_{\text{esc}} \approx 1 - 2$ per cent for the Milky Way galaxy. Such low values are not surprising since star forming regions are usually enshrouded in neutral gas with column density $N_{\text{HI}} \gtrsim 10^{20} \text{ cm}^{-2}$, three orders of magnitude higher than the value that yields an optical depth of $\tau = 1$ for ionising photons with energy 1 Rydberg; it is this neutral gas that fuels star formation in the first place. For galaxies to be able to reionise the Universe by $z \approx 6$ and provide the bulk of the ionising photons post-reionisation, f_{esc} needs to increase rapidly with redshift, $\propto (1+z)^{3.4}$ according to Haardt & Madau (2012) or even faster (Khaire et al. 2015). Such a rapid evolution of the escape fraction then suggests that the ISM/CGM of high- z galaxies is fundamentally different from that at low z ; the expected decrease in dust content is not enough to explain the trend. Why this should be so is a mystery whose resolution is key to understanding cosmological reionisation.

Whether the escape fraction indeed evolves (rapidly) can in principle be tested directly by measuring f_{esc} as function of redshift. There are currently no direct detections of ionising photons escaping from individual galaxies at $z \approx 1$ (Bridge et al. 2010; Siana et al. 2010; Rutkowski et al. 2015), with 3 σ upper limits of $f_{\text{esc}} \approx 2$ per cent. In contrast, Nestor et al. (2013) measure $f_{\text{esc}} = 5 - 7$ per cent for $z \approx 3$ Lyman-break galaxies (see also

* mahavir.sharma@durham.ac.uk

Vanzella et al. 2012) and even higher values for Lyman- α emitters. These values are significantly higher than more recent determination of a value < 2 per cent by Grazian et al. (2015) for LBGs at $3.3 < z < 4$. The observational evidence for evolution in f_{esc} is thus currently inconclusive.

Numerical simulations of galaxy formation that include radiative transfer, aimed at calculating f_{esc} at $z \gtrsim 6$, also yield contradictory results. Kimm & Cen (2014) quote values of $f_{\text{esc}} \approx 10$ per cent, with even higher values of ≈ 20 per cent during starbursts. Paardekooper et al. (2015) find much lower values, and claim that f_{esc} decreases rapidly with halo mass and cosmic time (see also Yajima et al. 2011; Razoumov & Sommer-Larsen 2010; Wise et al. 2014). In contrast, Ma et al. (2015) find intermediate values, $f_{\text{esc}} \approx 5$ per cent, with no strong dependence on either galaxy mass or cosmic time. Most ionising photons that do not make it out of their natal galaxy are absorbed locally - within several tens of parsecs of the star that emitted them. Consequently, the level of discrepancy between current simulations is not surprising, since the detailed properties of the ISM need to be modelled very accurately, with little guidance from observations.

A generic feature of these radiative transfer simulations is that starbursts clear channels in the ISM through which ionising photons escape (e.g. Fujita et al. 2003), a phenomenon that is particularly efficient at $z \gtrsim 6$ when galaxies are particularly bursty (e.g. Wise & Abel 2008) and drive winds. Heckman (2001) uses X-ray and optical emission line data to conclude that winds occur in galaxies with star formation surface density above a critical value of $\dot{\Sigma}_{*,\text{crit}} \approx 0.1 \text{ M}_{\odot} \text{ yr}^{-1} \text{ kpc}^{-2}$. Theoretical models of outflows driven by starbursts through supernovae (Clarke & Oey 2002), radiation pressure (Murray et al. 2011) or turbulent stirring (Scannapieco et al. 2012), support the existence of such a threshold, at similar values of $\dot{\Sigma}_{*,\text{crit}}$ as inferred from observations.

If the lifetime of massive stars is shorter than the time required to create channels in the ISM, then the fraction of all ionising photons that escapes from a galaxy may be small, even though f_{esc} is high once the channels have been created (Kimm & Cen 2014). Compact starbursts may suffer less from such a timescale mismatch. Indeed, a wind moving with speed $v \gtrsim 100 \text{ km s}^{-1}$ can carve a 500 pc wide channel in a time $\leq 5 \text{ Myr}$, comparable to the typical lifetime of a massive star. The few observed cases with large emissivities indeed result from very compact starbursts. Borthakur et al. (2014) and Izotov et al. (2016) find $f_{\text{esc}} \approx 20$ and 8 per cent, respectively, in $z \approx 0.2 - 0.3$ compact starbursts; de Barros et al. (2015) find a relative escape fraction of 60 per cent in a $z \approx 3$ compact starburst, and there is tantalising evidence that photons escape in channels (e.g. Chen et al. 2007; Zastrow et al. 2013).

Here we propose a model in which f_{esc} for a star forming region depends on the local star formation surface density averaged on a scale of $\approx 1 \text{ kpc}^2$, $\dot{\Sigma}_{*}$, motivated by the arguments presented above. We assume that when $\dot{\Sigma}_{*} \geq \dot{\Sigma}_{*,\text{crit}}$ the escape fraction, f_{esc} , is constant and equal to $f_{\text{esc,max}}$ due to self-regulation of star formation. We take $f_{\text{esc,max}} \approx 0.2$, roughly the observed upper limit, but explore how our results change if $f_{\text{esc,max}}$ is varied between 0.1 and 0.4. When $\dot{\Sigma}_{*} < \dot{\Sigma}_{*,\text{crit}}$ we take $f_{\text{esc}} = 0$. We use this Ansatz to derive f_{esc} for all galaxies in the EAGLE simulation (Schaye et al. 2015; Crain et al. 2015). We do not perform radiative transfer on EAGLE galaxies directly since these simulations do not have enough resolution to model the physics that generates outflow driven channels.

In Section 2, we calculate how the escape fraction depends on luminosity and redshift, illustrate what this implies for reionisation, the amplitude of the ionising background below $z = 6$, and the

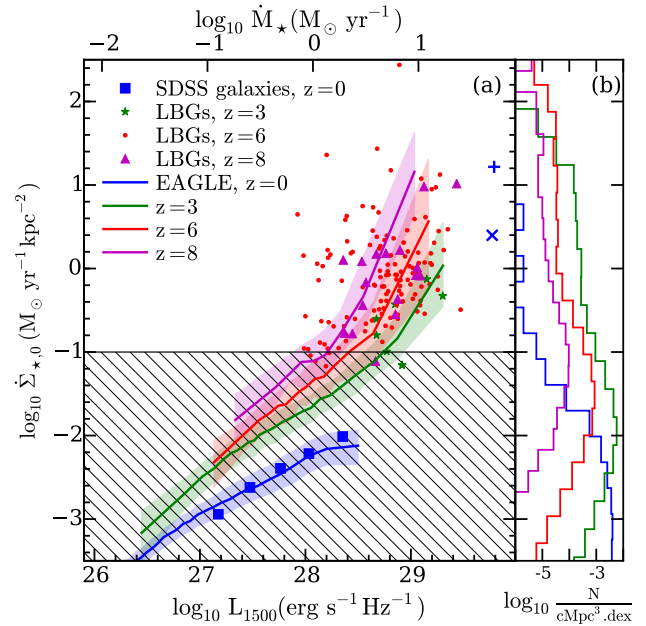


Figure 1. The dependence of the mean surface density of star formation, $\dot{\Sigma}_{*,0}$, on star formation rate and redshift. **Panel a:** $\dot{\Sigma}_{*,0}$ of EAGLE galaxies with stellar mass $> 10^8 \text{ M}_{\odot}$, as a function of their 1500Å UV luminosity (L_{1500} , bottom axis), corresponding star formation rate, \dot{M}_{*} , top axis), with coloured lines depicting the median relation, and coloured regions enclosing the 25th to 75th percentile range. Different colours refer to different redshifts (blue, $z = 0$, green, $z = 3$, red, $z = 6$, magenta, $z = 8$). $\dot{\Sigma}_{*,0}$ increases with \dot{M}_{*} at given z , and with z at given \dot{M}_{*} . Horizontal black line shows the critical star formation rate surface density ($\dot{\Sigma}_{*,\text{crit}}$) for outflows (Heckman 2001). **Panel b:** Number density of EAGLE galaxies in bins of $\dot{\Sigma}_{*,0}$, using the same colour scheme. At $z = 0$, galaxies with $\dot{\Sigma}_{*,0} \gtrsim \dot{\Sigma}_{*,\text{crit}}$ above which significant winds develop are present in the simulation, but they are very rare. However at $z \gtrsim 6$, most EAGLE galaxies with $\dot{M}_{*} > 1 \text{ M}_{\odot} \text{ yr}^{-1}$ are above this limit, and are expected to drive strong winds. Observed values of $\dot{\Sigma}_{*,0}$ are plotted in panel a, with colours depending on z matching those of the simulation; the region of low $\dot{\Sigma}_{*,0}$ where winds are not expected is hashed. The data shown are: $z = 0$, Sloan Digital Sky Survey measurements (Brisbin & Harwit 2012) (squares), the galaxies with high values of f_{esc} from Borthakur et al. (2014) (cross) and Izotov et al. (2016) (plus), Lyman-break galaxies from Giavalisco et al. (1996) at $z = 3$ (stars), from Curtis-Lake et al. (2014) at $z = 6$ (small red dots) and at $z = 8$ (triangles). EAGLE galaxies reproduce the dependence of $\dot{\Sigma}_{*,0}$ on \dot{M}_{*} and z .

nature of the galaxies that reionised the Universe. We summarise in Section 3.

2 ESCAPE OF IONISING PHOTONS FROM GALAXIES

2.1 The evolution of the star formation surface density

The EAGLE hydrodynamical cosmological simulations (Schaye et al. 2015; Crain et al. 2015) use subgrid modules for star and black hole formation, and feedback from stars and AGN. The star formation rate is calculated as function of pressure that ensures that galaxies follow the observed relation at $z = 0$ between gas surface density and $\dot{\Sigma}_{*}$ from Kennicutt (1998), as described in Schaye & Dalla Vecchia (2008), and the model assumes that this relation does not evolve. The star formation rate is assumed to be zero below

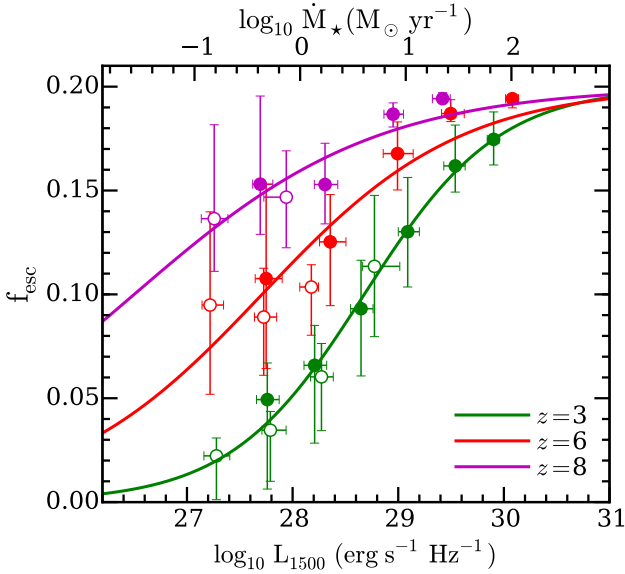


Figure 2. Mean inferred escape fraction for ionising photons (f_{esc}) from galaxies in EAGLE as a function of the 1500 Å luminosity (L_{1500}) at three redshifts (green: $z = 3$, red: $z = 6$, magenta: $z = 8$), for $f_{\text{esc,max}} = 0.2$. Circles represent the luminosity-weighted average of f_{esc} , with error bars encompassing the 25th to 75th percentile range. Filled circles refer to the reference simulation (labelled Ref-L0100N1504), open circles to the simulation that has eight times better mass resolution (labelled Recal-L0025N0752). Simulation results are fitted with a sigmoid function shown as solid curves. The escape fraction increases with luminosity and redshift.

the metallicity-dependent threshold of Schaye (2004). Gas particles are stochastically converted into star particles with a probability per unit time that depends on their star formation rate. The EAGLE suite includes models that vary in numerical resolution to test for convergence. Here we use two models, Ref-L0100N1504 (linear size $L = 100$ Mpc, gas particle mass $m_g = 1.81 \times 10^6 M_\odot$) and the higher resolution model Recal-L0025N0752 ($L = 25$ Mpc, $m_g = 2.26 \times 10^5 M_\odot$).

We compute f_{esc} of a galaxy by calculating the escape fraction of all its individual star-forming regions, and weighting them by their star formation rate. For an individual region we take $f_{\text{esc}} = f_{\text{esc,max}}$ when $\dot{\Sigma}_* \geq \dot{\Sigma}_{*,\text{crit}}$ and zero otherwise. Galaxies in EAGLE are both more active (higher \dot{M}_*/M_*) and smaller at earlier times. As a consequence, an increasing fraction of star-forming regions have higher ISM pressure (see Fig. 7 in Crain et al. 2015), which have higher $\dot{\Sigma}_*$ according to the star formation prescription of Schaye & Dalla Vecchia (2008), and hence higher f_{esc} as well.

The local quantity $\dot{\Sigma}_*$ cannot be compared directly to observations. We therefore compute $\dot{\Sigma}_{*,0} \equiv \dot{M}_*/(2\pi R_*^2)$, where \dot{M}_* is the star formation rate of the galaxy and R_* its half-mass radius; $\dot{\Sigma}_{*,0}$ is the central surface density of star formation if the disk is exponential. In EAGLE, $\dot{\Sigma}_{*,0}$ increases with \dot{M}_* at given redshift, and with redshift at given \dot{M}_* (coloured bands in Fig. 1). For example, for a galaxy with $\dot{M}_* = 1 M_\odot \text{ yr}^{-1}$, $\dot{\Sigma}_{*,0} = 10^{-2} M_\odot \text{ yr}^{-1} \text{ kpc}^{-2}$ at $z = 0$, but is more than a factor of 10 higher at $z = 8$. The histogram in Fig. 1 shows this more quantitatively.

Observed galaxies display a very similar dependence of $\dot{\Sigma}_{*,0}$ on \dot{M}_* and z as EAGLE galaxies (Fig. 1, data points are $\dot{\Sigma}_{*,0}$ as function of \dot{M}_* for observed galaxies, with colours depending on redshift in the same manner as the coloured bands representing EA-

GLE). That EAGLE reproduces these trends so well is consistent with the fact that the simulation reproduces separately the observed trend of increasing \dot{M}_*/M_* with z (Furlong et al. 2015a), and of decreasing size with z (Furlong et al. 2015b).

The strong evolution of the surface density of star formation suggests that an increasingly large fraction of galaxies drive winds at early times: whereas at $z = 0$ most galaxies have $\dot{\Sigma}_{*,0} \ll \dot{\Sigma}_{*,\text{crit}}$ and hence are not expected to drive winds (these are located in the hashed region in Fig. 1), at $z \gtrsim 6$ most galaxies have $\dot{\Sigma}_{*,0} \gtrsim \dot{\Sigma}_{*,\text{crit}}$ and their star-forming regions are expected to driven outflows.

A consequence of the rapid increase of $\dot{\Sigma}_{*,0}$ with z is that f_{esc} also increases rapidly with z , as shown in Fig. 2. Large values of f_{esc} are extremely rare at $z = 0$; at $z = 3$ only the very brightest galaxies have significant non-zero values of $f_{\text{esc}} \gtrsim 10$ per cent (in the absence of dust); but above $z = 6$ galaxies with $L_{1500} > 10^{28} \text{ erg s}^{-1} \text{ Hz}^{-1}$ have a mean $f_{\text{esc}} > 10$ per cent, which increases further to $f_{\text{esc}} > 15$ per cent by $z = 8$. There is good agreement (better than 10 per cent) in the predicted value of f_{esc} between models Ref-L0100N1504 and Recal-L0025N0752, that differ by a factor of 8 in mass resolution, for galaxies brighter than $10^{28} \text{ erg s}^{-1} \text{ Hz}^{-1}$. We use the higher resolution simulation to calculate f_{esc} for galaxies brighter than $10^{27} \text{ erg s}^{-1} \text{ Hz}^{-1}$.

Given the good agreement in the evolution of $\dot{\Sigma}_{*,0}$ between EAGLE and observed galaxies, we conclude that the increased activity in galaxies, coupled with their smaller sizes, implies that f_{esc} increases rapidly with redshift in observed galaxies as well. Such vigorously star forming galaxies are rare in the local Universe, but they do occur, both in the data and in the simulations which have a long tail to high $\dot{\Sigma}_{*,0}$ as shown by the blue histogram in Fig. 1. In fact, the blue cross and plus symbols correspond to the low- z galaxies identified by Borthakur et al. (2014) and Izotov et al. (2016) as having a high escape fraction corrected for dust of 20 and 8 per cent, respectively. (High redshift star-forming galaxies show no evidence of the presence of dust, Bouwens et al. 2015b.) These are located in a similar region in the $\dot{M}_* - \dot{\Sigma}_{*,0}$ plot of Fig. 1 as most of the currently detected brighter galaxies at $z \gtrsim 6$, and so we expect the latter to have similarly high values of f_{esc} . We investigate the consequences of a high escape fractions for galaxies with high values of $\dot{\Sigma}_*$ next.

2.2 The contribution of observed galaxies to reionisation

We can combine the dependence of the escape fraction on galaxy luminosity and redshift, $f_{\text{esc}}(L_{1500}, z)$, from Fig. 2 with the observed number density of galaxies as function of 1500Å luminosity from Bouwens et al. (2015a), $\Phi(L_{1500})$, to obtain the emissivity at energies 13.6 eV, $\epsilon = f_{\text{esc}}(L_\nu, z) \Phi(L_\nu, z) L(\nu_{\text{th}}, z)$, and the emissivity of ionising photons, $\dot{n}_{\gamma,\text{esc}}(L_{1500}, z) = f_{\text{esc}}(L_\nu, z) \Phi(L_\nu, z) \int_{\nu_{\text{th}}}^{\infty} \frac{L_\nu}{h\nu} d\nu$. Here, L_ν is the luminosity of the galaxy at a frequency ν and $h\nu_{\text{th}} = 13.6 \text{ eV}$ the ionisation potential of hydrogen. We use the luminosity function at 1500 Å from Bouwens et al. (2015a), and assume that the intrinsic spectrum of the ionising sources has a break of $L(912\text{Å})/L(1500\text{Å}) = 1/6$ as in the Starburst99 model¹ (Leitherer et al. 1999; Bruzual & Charlot 2003). Resulting values of ϵ and of the cumulative contribution to the emissivity of ionising photons, $\dot{n}_{\gamma,\text{esc}}(> L_{1500}, z)$, are plotted in Fig. 3.

¹ We use the observed luminosity function *without* dust correction, implicitly assuming that dust obscuration affects ionising and 1500Å photons in the same way. The absolute escape fraction is then smaller than the values we quote by the (small) dust correction.

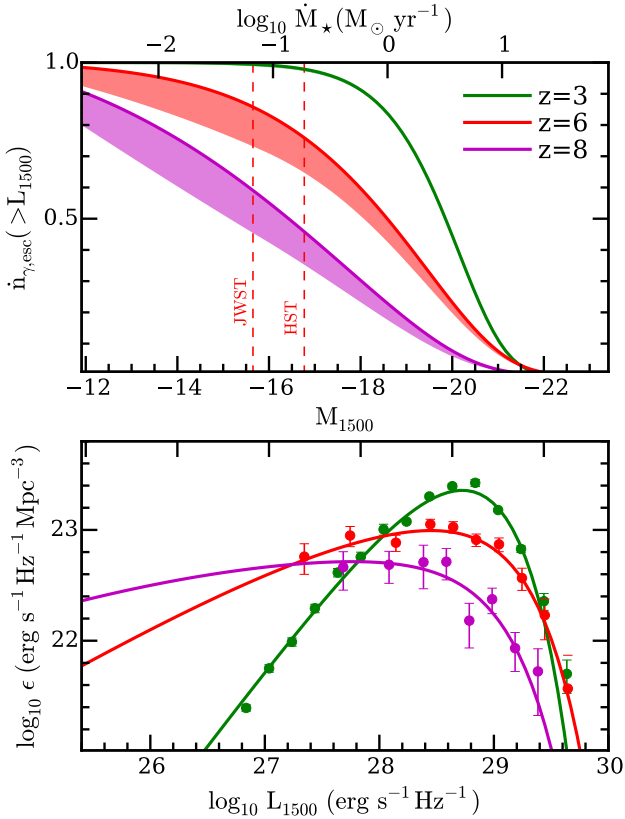


Figure 3. Detectability of the galaxies that reionised the Universe. **Bottom panel:** Emissivity at 912\AA (ϵ) as a function of the 1500\AA luminosity of galaxies (middle axis shows corresponding M_{1500} magnitude on the AB-system, top axis shows the corresponding star formation rate) for redshifts $z = 3$ (green), 6 (red) and 8 (magenta). Curves combine the observed luminosity function of galaxies from [Bouwens et al. \(2015a\)](#); [Parsa et al. \(2015\)](#), with model for the escape fraction of ionising photons described in the text. Even though the galaxy luminosity functions steepen rapidly towards higher redshifts, brighter galaxies dominate the emissivity even at $z = 8$. **Top panel:** Cumulative contribution of galaxies to the emissivity of ionising photons ($\dot{n}_{\gamma, \text{esc}}$) at the corresponding redshifts; the HST detection limit at $z = 6$ ([Bouwens et al. 2015a](#)) is shown as a red dashed line, the JWST detection limit for a 30 h integration is also indicated. The lower edge of the shaded region corresponds to using a constant value for f_{esc} for all galaxies fainter than $M_{1500} = -16$, and extrapolating the luminosity function to $M_{1500} = -10$.

At $z = 3$, the faint-end slope of the luminosity function is sufficiently flat that bright galaxies dominate both ϵ and the photon production rate. Interestingly, even though the luminosity function becomes much steeper at $z = 6$ and even more so at $z = 8$ ([Bouwens et al. 2015a](#)), bright galaxies still dominate at these earlier times, with 50 per cent of photons escaping from galaxies brighter than $M_{1500} = -18$ at $z = 6$, and $M_{1500} = -16.5$ at $z = 8$. This is because the escape fraction of galaxies drops with decreasing luminosity (Fig. 2) faster than that the number of such galaxies increases, even when luminosity function is very steep.

We show in Fig. 4 (bottom panel) that the evolution of the ionising emissivity, $\dot{n}_{\gamma, \text{esc}}$, is consistent with the latest constraints on reionisation ([Bouwens et al. 2015a](#), green band), and crucially, also with the emissivity required to produce the ionising background post-reionisation ([Becker & Bolton 2013](#), blue band). In the top

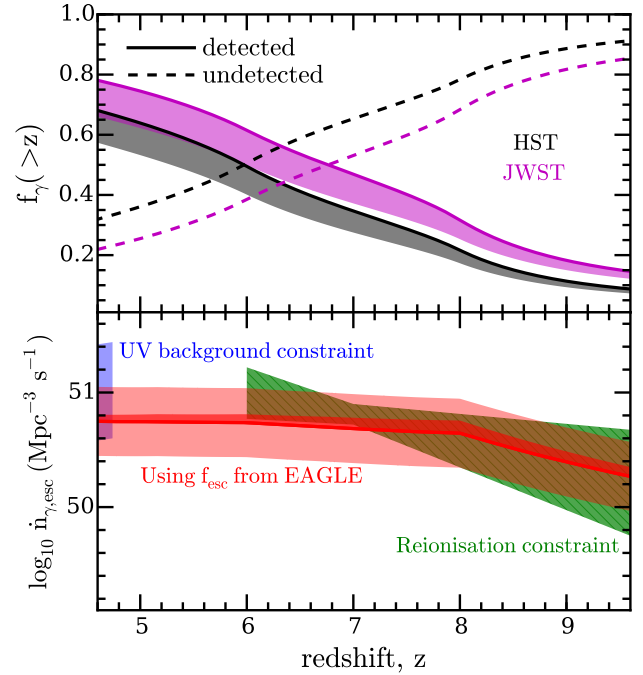


Figure 4. Total ionising emissivity ($\dot{n}_{\gamma, \text{esc}}$, **bottom panel**, solid red line) and fraction of that emissivity due to galaxies above a given detection limit ($f_{\gamma}(>z)$, **top panel**, HST: solid black; 30 hour JWST limit: solid magenta), obtained by integrating the emissivity as function of luminosity from Fig. 3. Shaded region (dark shaded region in the lower panel) shows the range if a constant value for f_{esc} is used for galaxies fainter than $M_{1500} = -16$, and the luminosity function is extrapolated to $M_{1500} = -10$. The light red shaded region in the bottom panel, shows the range of emissivity when the maximum allowed escape fraction is varied between 10 and 40 per cent. The blue shaded region represents the range in $\dot{n}_{\gamma, \text{esc}}$ required to match the amplitude of the UV-background ([Becker & Bolton 2013](#)); the green shaded region is the range required to match the Thomson optical depth and the evolution of the ionised volume fraction during reionisation ([Bouwens et al. 2015a](#)). In our model, galaxies emit enough ionising photons to match the reionisation constraints as well as the lower- z amplitude of the UV-background. In this scenario, 50% (60%) of these photons are emitted by galaxies above the HST (JWST) limit by $z = 6$ (see top panel).

we plot the cumulative fraction of ionising photons emitted up to a redshift z , $f_{\gamma}(>z)$, by the galaxies above the current detection limit of HST (black curve) and that predicted for a 30 hour JWST integration (magenta curve). Before $z = 6$, approximately 50 per cent of the photons that reionised the Universe escape from galaxies that are above the detection limit of the *Hubble Ultra Deep Field*. Therefore the Universe was reionised by relatively bright, vigorously star forming, compact galaxies.

3 SUMMARY AND CONCLUSION

The fraction of ionising photons that escapes from galaxies (f_{esc}) is a crucial ingredient in any theory of reionisation by galaxies. Observed values of f_{esc} at redshifts $z \gtrsim 1$ are small, $f_{\text{esc}} = 1 - 2$ per cent. This implies that, unless f_{esc} increases rapidly with redshift, reionisation was caused by a large population of faint galaxies, below the detection limit of the *Hubble Space Telescope* (HST) and possibly even below that of the *James Webb Space Telescope* (JWST). The existence of such a population is plausible, given the

measured steep faint-end slopes of $z \gtrsim 6$ luminosity functions (e.g. Bouwens et al. 2015b).

The escape fraction of photons from dust-free galaxies is mostly set by the structure of their interstellar medium, since ionising photons tend to be absorbed close to star forming region from which they originate. Strong winds, driven by supernovae and massive stars in a star forming region, are thought to create channels through which photons escape. Such winds tend to be observed when star formation occurs above a given surface density threshold (Heckman 2001), and in the few cases where photons are observed to escape in reasonable fractions of $f_{\text{esc}} \gtrsim 20$ per cent, the surface density of star formation is indeed very high (Borthakur et al. 2014; de Barros et al. 2015).

We present a model of reionisation that encapsulates these results, by assigning a 20 per cent escape fractions to photons emerging from young star forming regions with a high value above the $\dot{\Sigma}_{*,\text{crit}} = 0.1 M_{\odot} \text{ yr}^{-1} \text{ kpc}^{-2}$ threshold of Heckman (2001), and zero below this threshold. We computed the galaxy-averaged escape fraction as a function of luminosity and redshift by applying this criterion to individual gas particles in the EAGLE simulation, which reproduces the observed star formation rate surface densities as a function of luminosity. We find that luminosity weighted mean value of f_{esc} increases rapidly with redshift, reaching values in the range 5-20 per cent at $z = 6$ for galaxies above the HST detection limit, with the brighter galaxies having higher values. Combining this result with the observed luminosity function of galaxies from Bouwens et al. (2015a), we obtain a model that is consistent with the latest constraints on reionisation, and on the amplitude of the ionising background post-reionisation. In this model, the brighter sources dominate reionisation. In particular, we estimate that 50 per cent of the ionising photons that were emitted before $z = 6$ originated from galaxies above the *Hubble Ultra Deep Field* detection limit. The instantaneous emissivity of those galaxies is ≈ 70 per cent of the total emissivity at that redshift. JWST will be able to study these sources in detail.

ACKNOWLEDGMENTS

We thank the anonymous referee for insightful comments that improved this manuscript. We gratefully acknowledge the expert high performance computing support of Lydia Heck and Peter Draper. We thank PRACE for awarding us access to the Curie facility based in France at Trés Grand Centre de Calcul. This work used the DiRAC Data Centric system at Durham University, operated by the Institute for Computational Cosmology on behalf of the STFC DiRAC HPC Facility (www.dirac.ac.uk); this equipment was funded by BIS National E-infrastructure capital grant ST/K00042X/1, STFC capital grant ST/H008519/1, STFC DiRAC Operations grant ST/K003267/1 and Durham University. DiRAC is part of the National E-Infrastructure. The study was sponsored by the Dutch National Computing Facilities Foundation, with financial support from the NWO, the ERC Grant agreements 278594 GasAroundGalaxies, GA 267291 Cosmiway, the Interuniversity Attraction Poles Programme initiated by the Belgian Science Policy Office ([AP P7/08 CHARMI]), and the UK STFC (grant numbers ST/F001166/1 and ST/I000976/1). RAC is a Royal Society University Research Fellow. M.Sharma is an STFC Post-doctoral fellow at the ICC.

REFERENCES

Becker G. D., Bolton J. S., 2013, MNRAS, 436, 1023

MNRAS **000**, ??-?? (2014)

- Bland-Hawthorn J., Maloney P. R., 2001, ApJ, 550, L231
 Borthakur S., Heckman T. M., Leitherer C., Overzier R. A., 2014, Science, 346, 216
 Bouwens R. J., Illingworth G. D., Oesch P. A., Caruana J., Holwerda B., Smit R., Wilkins S., 2015a, ArXiv e-prints : 1503.08228
 Bouwens R. J. et al., 2011, ApJ, 737, 90
 Bouwens R. J. et al., 2015b, ApJ, 803, 34
 Bridge C. R. et al., 2010, ApJ, 720, 465
 Brisbin D., Harwit M., 2012, ApJ, 750, 142
 Bruzual G., Charlot S., 2003, MNRAS, 344, 1000
 Chen H.-W., Prochaska J. X., Gnedin N. Y., 2007, ApJ, 667, L125
 Clarke C., Oey M. S., 2002, MNRAS, 337, 1299
 Crain R. A. et al., 2015, MNRAS, 450, 1937
 Curtis-Lake E. et al., 2014, ArXiv e-prints : 1409.1832
 de Barros S. et al., 2015, ArXiv e-prints : 1507.06648
 Ferrara A., Loeb A., 2013, MNRAS, 431, 2826
 Fujita A., Martin C. L., Mac Low M.-M., Abel T., 2003, ApJ, 599, 50
 Furlong M. et al., 2015a, ArXiv e-prints : 1510.05645
 Furlong M. et al., 2015b, MNRAS
 Gialalisco M., Steidel C. C., Macchetto F. D., 1996, ApJ, 470, 189
 Gnedin N. Y., 2000, ApJ, 535, 530
 Grazian A. et al., 2015, ArXiv e-prints : 1509.01101
 Haardt F., Madau P., 2012, ApJ, 746, 125
 Heckman T. M., 2001, in Astronomical Society of the Pacific Conference Series, Vol. 240, Gas and Galaxy Evolution, Hibbard J. E., Rupen M., van Gorkom J. H., eds., p. 345
 Heckman T. M. et al., 2011, ApJ, 730, 5
 Izotov Y. I., Orlitova I., Schaerer D., Thuan T. X., Verhamme A., Guseva N., Worseck G., 2016, Nature, ArXiv e-prints : 1601.03068
 Kennicutt, Jr. R. C., 1998, ARA&A, 36, 189
 Khaire V., Srikanth R., Choudhury T. R., Gaikwad P., 2015, ArXiv e-prints : 1510.04700
 Kimm T., Cen R., 2014, ApJ, 788, 121
 Leitherer C. et al., 1999, ApJS, 123, 3
 Loeb A., Barkana R., 2001, ARA&A, 39, 19
 Ma X., Kasen D., Hopkins P. F., Faucher-Giguère C.-A., Quataert E., Kereš D., Murray N., 2015, MNRAS, 453, 960
 McGreer I. D., Mesinger A., D'Odorico V., 2015, MNRAS, 447, 499
 Mitra S., Choudhury T. R., Ferrara A., 2015, ArXiv e-prints
 Murray N., Ménard B., Thompson T. A., 2011, ApJ, 735, 66
 Nestor D. B., Shapley A. E., Kornei K. A., Steidel C. C., Siana B., 2013, ApJ, 765, 47
 Paardekooper J.-P., Khochfar S., Dalla Vecchia C., 2015, MNRAS, 451, 2544
 Parsa S., Dunlop J. S., McLure R. J., Mortlock A., 2015, ArXiv e-prints : 1507.05629
 Razoumov A. O., Sommer-Larsen J., 2010, ApJ, 710, 1239
 Robertson B. E., Ellis R. S., Furlanetto S. R., Dunlop J. S., 2015, ApJ, 802, L19
 Robertson B. E. et al., 2013, ApJ, 768, 71
 Rutkowski M. J. et al., 2015, ArXiv e-prints : 1511.01998
 Scannapieco E., Gray W. J., Pan L., 2012, ApJ, 746, 57
 Schaye J., 2004, ApJ, 609, 667
 Schaye J. et al., 2015, MNRAS, 446, 521
 Schaye J., Dalla Vecchia C., 2008, MNRAS, 383, 1210
 Shin M.-S., Trac H., Cen R., 2008, ApJ, 681, 756
 Siana B. et al., 2010, ApJ, 723, 241
 Vanzella E. et al., 2012, ApJ, 751, 70
 Wise J. H., Abel T., 2008, ApJ, 685, 40
 Wise J. H., Demchenko V. G., Halicek M. T., Norman M. L., Turk M. J., Abel T., Smith B. D., 2014, MNRAS, 442, 2560
 Yajima H., Choi J.-H., Nagamine K., 2011, MNRAS, 412, 411
 Zastrow J., Oey M. S., Veilleux S., McDonald M., 2013, ApJ, 779, 76